High Power Laser Science and Engineering, (2017), Vol. 5, e13, 6 pages.

doi:10.1017/hpl.2017.13

Laser-induced microstructures on silicon for laser-driven acceleration experiments

Tina Ebert, Nico W. Neumann, Torsten Abel, Gabriel Schaumann, and Markus Roth

Department of Nuclear Physics, TU Darmstadt, Germany

(Received 30 October 2016; revised 26 February 2017; accepted 5 May 2017)

Abstract

Ultrashort laser pulses are used to create surface structures on thin (25 μm) silicon (Si) wafers. Scanning the wafer with a galvanometric mirror system creates large homogeneously structured areas. The variety of structure shapes that can be generated with this method is exemplified by the analysis of shape, height and distance of structures created in the ambient media air and isopropanol. A study of the correlation between structure height and remaining wafer thickness is presented. The comparatively easy manufacturing technique and the structure variety that allows for custom-tailored targets show great potential for high repetition rate ion acceleration experiments.

Keywords: microstructured targets; black silicon; ion acceleration

1. Introduction

Over the last decade, the interaction of high-intensity laser fields with thin solid targets has attracted a great deal of attention due to its wide field of application. During the interaction process high-energy electrons are emitted[1]. These 'hot electrons' also give rise to an emission of x-rays[2] and high-energy ion beams[3, 4]. One of the underlying mechanisms is the target normal sheath acceleration (TNSA), where the heated electrons lead to a charge separation that creates strong electrostatic fields accelerating the ions[5]. To increase the number and energy of the hot electrons much effort has been spent on the improvement of the conversion efficiency of laser energy into hot electron energy. To foster conversion efficiency, not only the laser parameters, i.e., laser intensity, pulse duration and energy, but also the target design can be tuned[6–8].

Recent theoretical studies have shown that modifications of the front surface of the targets improve both laser absorption, hence an increased number and energy of the hot electrons, and collimation of the emitted ion beam by guiding effects[6, 7]. Supplementary experimental work with nano-wire[8] and nano-brush[9] targets confirm these results and also show a suppressed plasma expansion on the front side of the target.

There exist various methods to create these surface structures such as electrochemical etching[10], microcontact printing[11], optical[12] and electron beam lithography[13], chemical vapor deposition[14] or short-pulse laser treatment[15, 16]. The latter has multiple advantages, including the possibility to create a wide range of structure variations. Once the laser system is set up, this method is also comparatively time- and cost-efficient. Along with different metals like Cu and Al the processing of crystalline silicon (Si) samples was studied intensively in the last two decades[17–19]. Here, a flat Si surface is processed with a femtosecond-pulsed laser resulting in conical spikes of different height, distance and shape depending on the laser fluence, the number of incident laser pulses, the wavelength, the pulse duration and the ambient medium. It is commonly assumed that these structures are generated by an interference of the incoming and the scattered light and the excitation of surface plasmon-polaritons. The laser–solid interaction causes the electrons and the lattice to heat rapidly. Depending on the laser pulse intensity this results in melting and rapid solidification of the surface or in an ablation of surface atoms. Even though the underlying processes are not completely understood yet, the method can be applied and the influences of the different parameters can be analyzed. Respective studies showed that processing in air or vacuum creates blunt spikes on a micrometer scale, whereas ambient gases containing sulfur result in sharper spikes[20]. If liquid media like water or alcohol are chosen, the structures are smaller and smoother[21]. This wide variety can be exploited to create custom-shaped structures for laser acceleration experiments.

So far, microstructured Si has found its main application in the solar industry because it enhances the light absorption in

Correspondence to: T. Ebert Email: tebert@ikp.tu-darmstadt.de

the complete spectrum emitted by the Sun[15]. The higher absorption is explained to be due to an increased surface area, the high aspect ratio of the cones trapping the light and a modified band gap as a result of doping the surface with ambient atoms. But Si is also a desirable choice as target material for laser acceleration experiments because it is easily available, comparatively cheap and easy to handle. The amount of fabricated targets can be upscaled without much effort once the parameters are set. Therefore, the technique is suitable for the target production for high repetition laser ion acceleration experiments. In this case, the individual targets would have to be placed on a suitable mount to prevent them from shock damage. If needed, it can be coated with thin layers of different materials like Au or Ni on both sides (flat and structured).

This paper presents a comparative study of short-pulse laser structured Si in air and alcohol with special focus on the different shapes and heights of the cones. To our knowledge, it is the first time that this was done on very thin Si wafers (approx. 25 µm) to be employed in laser-driven acceleration experiments. The results demonstrate the enormous potential of short-pulse laser structuring for custom-tailored solid targets.

2. Experimental setup

The microstructuring experiments described in this paper were conducted using an amplified Ti:sapphire laser system (KMLabs Inc.) with a central wavelength of 800 nm, a pulse duration of 100 fs and a repetition rate of 5 kHz. The power was adjusted by a combination of a waveplate and a polarizer and could be varied continuously in between 50 and 800 mW. The laser had a spatially Gaussian beam shape and was linearly polarized.

For all experiments crystalline Si samples with a thickness of 25 µm and a ⟨100⟩ surface orientation were used. To simplify the handling, these thin membranes were enclosed by a thicker frame (600 µm) and attached to a scanning electron microscope (SEM) holder pin (Figure 1). This pin was then placed in one of the processing chambers, which vary for different ambient media.

Figure 2 shows schematics of the two different processing chambers. In both setups the laser enters the chamber from above and impinges perpendicular on the Si sample surface. For microstructuring in air [Figure 2(a)], an open chamber with no extra supplements was chosen. To keep a constant filling level while microstructuring in fluid ambient media, a plate capacitor was added [Figure 2(b)]. A continuous capacity measurement provides information about the variation of the fluid amount during the process, which allows to keep the level constant.

To create larger structured areas the sample was scanned by the laser using a galvanometric two-mirror system. The wafers crystal orientation relative to the scan direction has

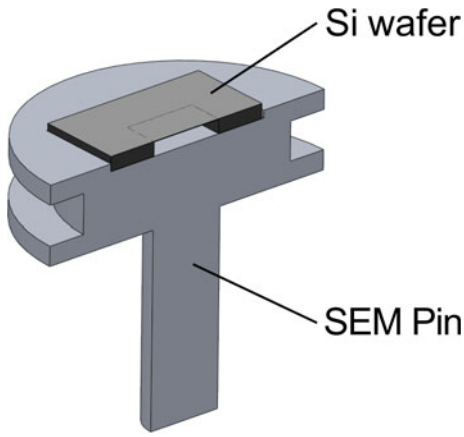

Figure 1. Sectional view of the Si wafer attached to an SEM pin for processing.

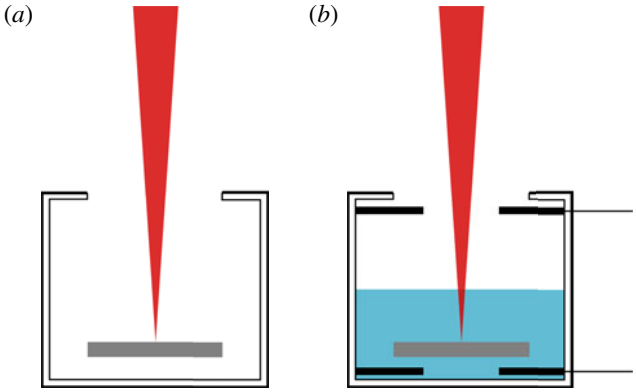

Figure 2. The setups for the two employed ambient media. Setup (a) was used for processing in air and setup (b) for processing in fluid ambient media. The latter has an additional plate capacitor to monitor the fluid level.

no influence on the structures, so the initial positioning can be arbitrary. The velocity and step size depend on the ambient medium. Typically, the velocity was varied in between 0.5 and 2 mm/s and the optimal step distance was in between 40% and 70% of the focal spot diameter. The position of the best focus was determined by varying the distance between focusing lens (300 mm focal length) and sample surface, thereby identifying the smallest focal spot size on the surface. For the structuring process this best focus was then placed slightly below the crystalline Si surface to prevent a plasma ignition before the laser hits the surface. With a focal spot size of (70 ± 5) µm the laser fluence at the sample surface could be tuned in between 4 and 10 kJ/m^2. All samples were characterized using images taken by an SEM (Phillips XL30 FEG) with different angles.

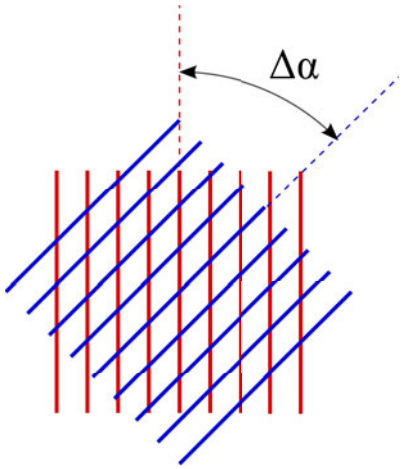

Figure 3. Schematic showing the rotation of the laser scanning raster used to create more homogeneous structures.

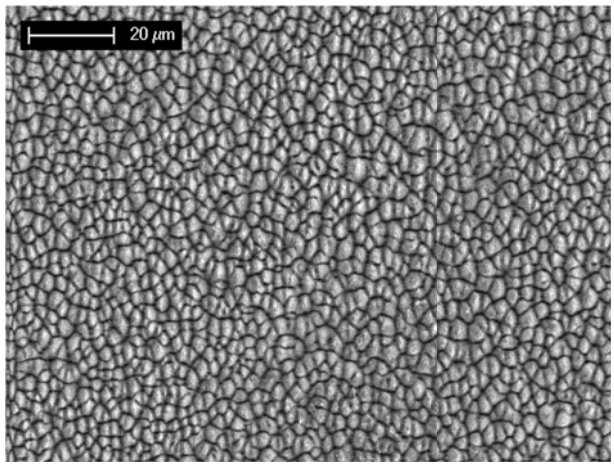

Figure 4. Si target structured in isopropanol with 1400 pulses at a fluence of 5.7 kJ/m^2 viewed from above with a 1500 × magnification.

3. Results

The galvanometric mirror system is used to structure large areas by scanning the surface with the laser focus. A typical size of such a rectangular area is 1 mm × 1 mm. The laser scans the probe line by line with a distance Δd between the lines. To achieve a high homogeneity this distance Δd has to be chosen carefully, depending on the laser focus size and the ambient medium. The number of pulses that hit one spot at the surface can be varied by altering the speed or the number of scans. To increase the homogeneity the scanning direction is rotated by an angle $\Delta\alpha$ after a full scan of the area, as can be seen in Figure 3. The number of rotations depends on the desired total number of pulses.

The result of this scanning procedure is a homogeneously structured target surface as can be seen in Figure 4. Here, the distance was set to $\Delta d = 40$ μm while having a focus size of 70 μm. The overlap has to be determined experimentally, since the employed focal camera measures the $1/e^2$ spot size, but the line width on the Si surface is influenced by the melting threshold of the material and therefore varies with intensity. If the distance is smaller than the optimum, the large overlap results in pile ups in between the lines. In case the distance is wider, unstructured gaps appear between the lines where the fluence was not high enough to create structures.

Depending on the ambient medium used during the structuring process the structures have a different shape and size. Figure 5 shows structures generated in air (left column) and in liquid isopropanol (right column). The structures generated in air have a height of approximately 15 μm and are therefore larger than the ones created in isopropanol, which are approximately 4 μm tall.

The top row of Figure 5 is viewed from above and shows that the structures created in air have an almost round base, whereas the bases of the structures generated in isopropanol are clearly more angular. Also, the isopropanol structures are separated by a rift of constant width unlike the air structures, that are more disordered. The difference in size also appears in the average distance between the structures which is about 10 μm in air and about 3 μm in isopropanol.

A side view is displayed in the bottom row of Figure 5. The images were taken under a viewing angle of 45°. The structures created in air look needle-like with a steep slope whereas the isopropanol structures are more cone-like with broader slopes. The needles are covered with a light fluff and the cones with small beads. This might be explained by the phases of the media which have different heat conduction properties.

Besides studying the shape variation in different ambient media the correlation of structure height and remaining substrate thickness was examined, which is of special interest for thin targets used in the scope of laser-induced particle acceleration. Figure 6 shows a sketch of the target buildup with the definitions for the structure height s and the base height b.

For this study the Si wafer was scanned in liquid isopropanol with a laser fluence of 5.7 kJ/m^2 with 700, 1400, 1750 and 2100 pulses. This meant 2, 4, 5 and 6 rotations of the scanning direction with a rotation angle of $\Delta\alpha = 45°$, respectively, since one full scan attributes 350 pulses. Figure 7 shows 90° side views of the four steps. Parts of the structured target area broke in the sixth rotation when 2100 pulses were applied. The reason for that is that there is almost no base left as can be seen in Figure 7(d). The values for structure and base heights are plotted in Figure 8. With increasing number of pulses the structure height increases whereas the base height decreases. Both correlations are

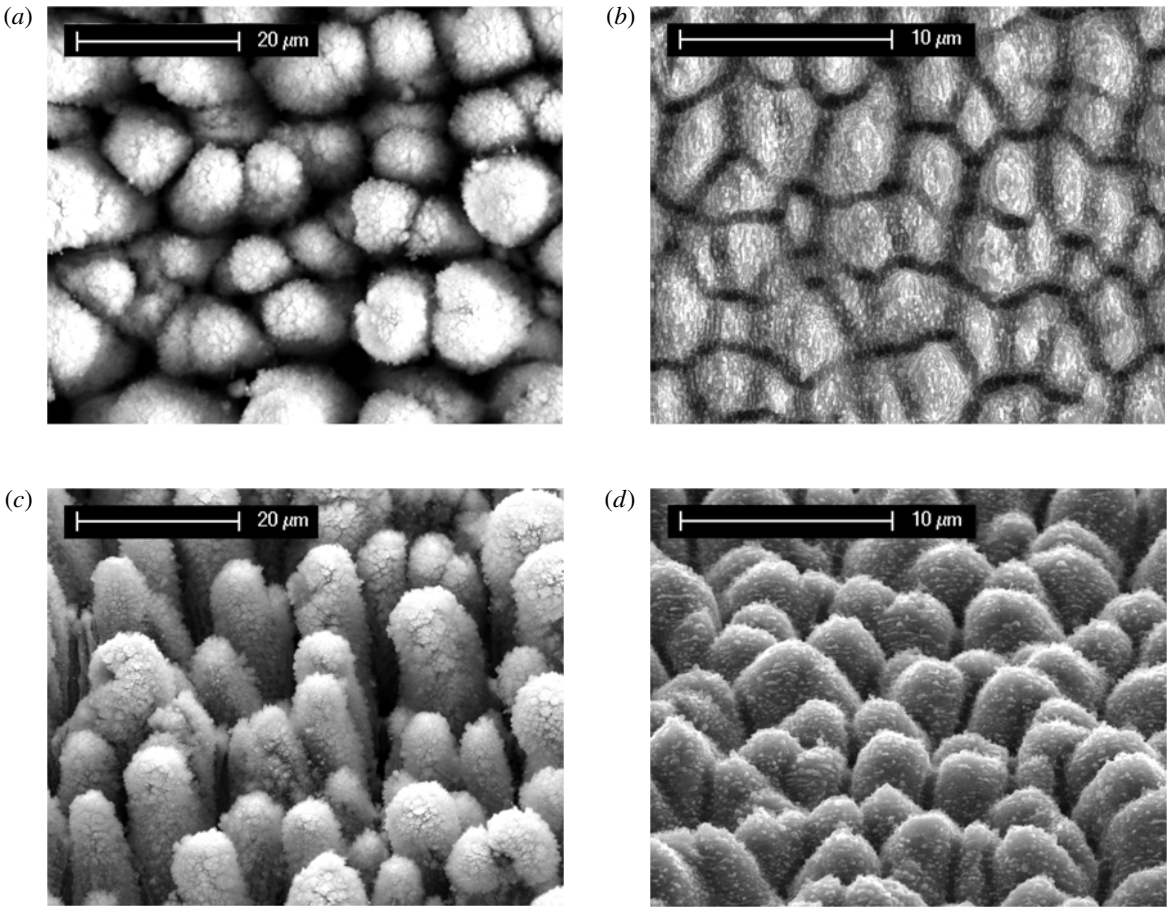

Figure 5. Comparison of the structure shapes resulting from different ambient media. The structures in the left column (images (a) and (c)) were created in air (8.6 kJ/m^2, 450 pulses) whereas the cones displayed in the right column (images (b) and (d)) were generated in isopropanol (5.7 kJ/m^2, 1400 pulses). The top row (images (a) and (b)) is viewed from above (0°) while the bottom row (images (c) and (d)) is viewed from the side (45°).

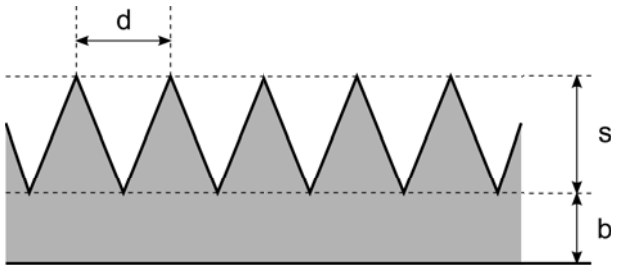

Figure 6. Sketch of the target buildup defining the three basic dimensions d, b and s, describing the cone distance, the base and the structure height, respectively.

nonlinear. If taller cones or needles with a thicker base height are required a different initial wafer thickness needs to be chosen. The results presented in this paper are summarized in Table 1.

Table 1. Approximate dimensions of structured Si regarding the height and distance of the cones in different ambient media.

	Structure comparison	
Ambient Medium	Structure height (µm)	Structure distance (µm)
Air	10–19	10
C_3H_8O	2–6	3

4. Summary

In summary, thin Si wafers are microstructured using femtosecond laser pulses in both air and isopropanol. The different characteristics of these structures are discussed. Although the spatial distribution of the structures is random, the shapes, heights and distances can be controlled by choosing the right parameter set of laser fluence, number of incident pulses and ambient medium. Furthermore, the ratio of structure height and remaining substrate thickness can be influenced. The processing method can be easily applied

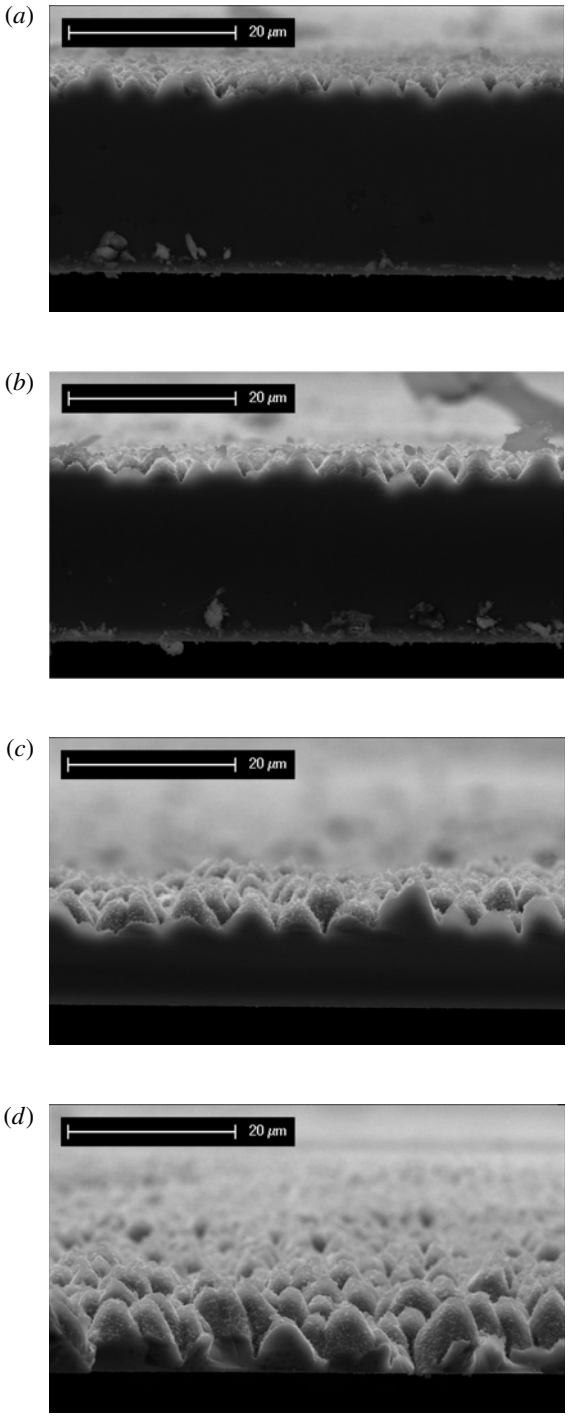

Figure 7. Si wafers processed in liquid isopropanol from an approximate 90° degree side view. The number of pulses were (a) 700, (b) 1400, (c) 1750 and (d) 2100 respectively, with a constant rotation angle of $\Delta\alpha = 45°$. The laser fluence of 5.7 kJ/m^2 was kept the same.

to large areas and is shown to create a homogeneously structured surface.

Altogether, laser-induced surface structures on thin Si substrates show a great potential as targets for high repetition rate ion acceleration experiments.

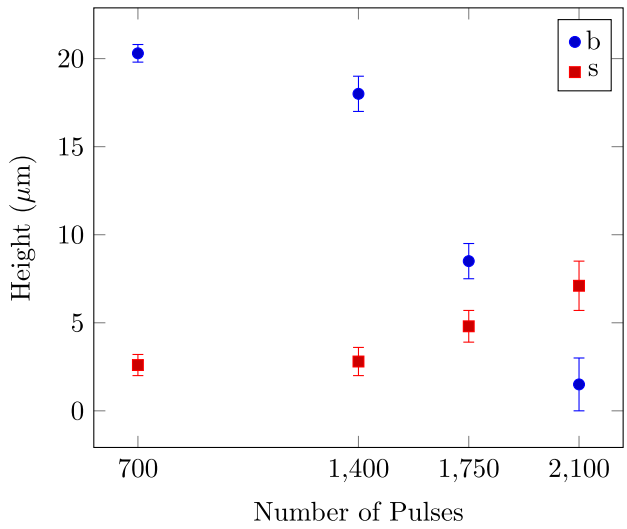

Figure 8. Correlation of remaining substrate thickness b and structure height s for different numbers of pulses. The laser fluence of 5.7 kJ/m^2 and the rotation angle of $\Delta\alpha = 45°$ were kept constant, as well as the ambient medium, which was isopropanol in all cases.

Acknowledgements

This work received financial support by the DFG in the framework of the Excellence Initiative, Darmstadt Graduate School of Excellence Energy Science and Engineering (GSC 1070). The authors thank the target laboratory of the Nuclear Physics Department, TU Darmstadt, for their support.

References

1. R. A. Snavely, M. H. Key, S. P. Hatchett, T. E. Cowan, M. Roth, T. W. Phillips, M. A. Stoyer, E. A. Henry, T. C. Sangster, M. S. Singh, S. C. Wilks, A. MacKinnon, A. Offenberger, D. M. Pennington, K. Yasuike, A. B. Langdon, B. F. Lasinski, J. Johnson, M. D. Perry, and E. M. Campbell, Phys. Rev. Lett. **85**, 14 (2000).
2. J. D. Kmetec, C. L. Gordon, J. J. Macklin, B. E. Lemoff, G. S. Brown, and S. E. Harris, Phys. Rev. Lett. **68**, 10 (1992).
3. S. P. Hatchett, C. G. Brown, T. E. Cowan, E. A. Henry, J. S. Johnson, M. H. Key, J. A. Koch, A. B. Langdon, B. F. Lasinski, R. W. Lee, A. J. Mackinnon, D. M. Pennington, M. D. Perry, T. W. Phillips, M. Roth, T. C. Sangster, M. S. Singh, R. A. Snavely, M. A. Stoyer, S. C. Wilks, and K. Yasuike, Phys. Plasmas **7**, 2076 (2000).
4. M. Roth and M. Schollmeier, CERN Yellow Reports **1**, 231 (2016).
5. S. C. Wilks, A. B. Langdon, T. E. Cowan, M. Roth, M. Singh, S. Hatchett, M. H. Key, D. Pennington, A. MacKinnon, and R. A. Snavely, Phys. Plasmas **8**, 2 (2001).
6. S. Jiang, A. G. Krygier, D. W. Schumacher, K. U. Akli, and R. R. Freeman, Phys. Rev. E. Stat. Nonlin. Soft Matter Phys. **89**, 1 (2014).
7. A. Andreev, N. Kumar, K. Platonov, and A. Pukhov, Phys. Plasmas **18**, 10 (2011).
8. H. Habara, S. Honda, M. Katayama, H. Sakagami, K. Nagai, and K. A. Tanaka, Phys. Plasmas **23**, 6 (2016).

9. Z. Zhao, L. Cao, L. Cao, J. Wang, W. Huang, W. Jiang, Y. He, Y. Wu, B. Zhu, K. Dong, Y. Ding, B. Zhang, Y. Gu, M. Y. Yu, and X. T. He, Phys. Plasmas **17**, 12 (2010).
10. D. Zhuang and J. H. Edgar, Mater. Sci. Eng. R Reports **48**, 1 (2005).
11. J. L. Wilbur, A. Kumar, E. Kim, and G. M. Whitesides, Adv. Mater. **6**, 7 (1994).
12. C. Mack, *Fundamental Principles of Optical Litography: The Science of Microfabrication* (John Wiley & Sons, 2008).
13. A. A. Tseng, K. Chen, C. D. Chen, and K. J. Ma, IEEE Trans. Electron. Packag. Manuf. **26**, 2 (2003).
14. J. Kong, A. M. Cassell, and H. Dai, Chem. Phys. Lett. **292**, 4 (1998).
15. X. Liu, P. R. Coxon, M. Peters, B. Hoex, J. M. Cole, and D. J. Fray, Energy Environ. Sci. **7**, 10 (2014).
16. B. R. Tull, J. E. Carey, E. Mazur, J. P. McDonald, and S. M. Yalisove, MRS Bull. **31**, 8 (2006).
17. T. Her, R. J. Finlay, C. Wu, S. Deliwala, and E. Mazur, Appl. Phys. Lett. **73**, 12 (1998).
18. M. Huang, F. Zhao, Y. Cheng, N. Xu, and Z. Xu, ACS Nano **3**, 12 (2009).
19. B. K. Nayak and M. C. Gupta, Opt. Lasers Eng. **48**, 10 (2010).
20. M. A. Sheehy, L. Winston, J. E. Carey, C. M. Friend, and E. Mazur, Chem. Mater. **17**, 14 (2005).
21. H. Liu, F. Chen, X. Wang, Q. Yang, H. Bian, J. Si, and X. Hou, Thin Solid Films **518**, 18 (2010).